Inorganic Chemistry

ARTICLE

pubs.acs.org/IC

Theoretical Analysis of Spin Crossover in Iron(II) [2 × 2] Molecular Grids

Ekaterina M. Zueva,*[,†] Elmira R. Ryabikh,[†] and Serguei A. Borshch*[,‡]

[†]Department of Inorganic Chemistry, Kazan State Technological University, 68 K. Marx Street, 420015 Kazan, Russia

[‡]Laboratoire de Chimie, UMR 5182, Ecole Normale Supérieure de Lyon, 46 allée d'Italie, 69364 Lyon Cedex 07, France

Supporting Information

ABSTRACT: We use quantum-chemical density functional theory calculations to elucidate the origin of spin-crossover pathways in two iron(II) [2 × 2] molecular grids with carbohydrazide-based bridging ligands. The complexes are characterized energetically and structurally in five available spin states. Special attention is paid to analysis of the structural distortion induced on each iron center by spin transition on any of its neighbors. The evolution of coordination polyhedra is monitored using the Continuous Shape Measures. It is demonstrated that a succession of spin transitions on different centers depends on the character of the induced distortion, either approaching or getting them away from a more regular low-spin geometry. These effects, resulting from the elasticity of bridging ligands, can be modulated by weak perturbations such as a change of the positions of the hydrogen atoms.

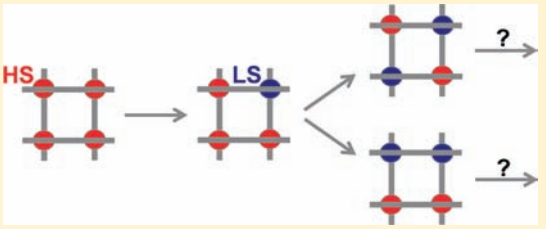

INTRODUCTION

Self-assembly strategies open ways to numerous nanosized molecular architectures displaying functional (catalytic, electrochemical, photoactive, magnetic, etc.) or multifunctional properties. Molecular grid-type systems seem to be especially interesting for molecular electronic applications because they can form monolayer structures on substrate surfaces. The spin-crossover (SCO) phenomenon[1] is one of the potentially valuable intrinsic properties already observed in iron(II) [2 × 2] grids.[2−5] An interesting feature of tetranuclear clusters appears because of the existence of five magnetic levels associated with the different numbers of high-spin (HS) and low-spin (LS) centers in the $(Fe_{HS})_n(Fe_{LS})_{4-n}$ (n = 0−4) cluster. Transitions between these levels can be considered as a manifestation of multistability, which replaces the well-known bistability of mononuclear SCO systems.

The family of [2 × 2] grid-type SCO complexes consists of species, in which four iron(II) centers are bridged by four extended organic ligands.[2−5] The latter are arranged in roughly parallel and eclipsed pairs above and below the pseudoplane of the four iron centers, whereas these pairs are aligned in almost perpendicular directions. Each iron center is surrounded by two tridentate moieties from different ligands, which form two fused five-membered metallacycles. In the reported complexes, the four iron centers are in a pseudooctahedral environment, either N_6[2,5] or N_4O_2.[3,4] The first grids of this type, reported by Lehn et al.,[2] comprise pyrimidine-based ligands and show continuous and incomplete thermal SCO between the $(Fe_{HS})_3(Fe_{LS})_1$ and $(Fe_{HS})_1(Fe_{LS})_3$ states. Recently, Meyer et al.[5] designed a rigid pyrazole-based ligand, with the pyrazole central moiety instead of the 2-methylpyrimidine or 2-phenylpyrimidine ones encountered in the previous case, and presented a compact grid containing the relatively short pyrazolate bridges. Interestingly, the pyrazolate-bridged grid resides in the $(Fe_{HS})_4$ state at room temperature and undergoes a continuous but complete SCO on the first site and then a partial SCO on the second one upon cooling.

Even more compact grids, where the neighboring iron centers are bridged by the single oxygen atoms, were reported by Sato et al.[3] and Thompson et al.[4] These grids comprise monodeprotonated carbohydrazide-based ligands (see Scheme 1). At room temperature, $[Fe_4(HL^{Ph})_4]^{4+}$ (**1**) and $[Fe_4(HL^{Me})_4]^{4+}$ (**2**) reside in the $(Fe_{HS})_4$ state, but despite the similarity in the molecular structures, they exhibit different behaviors upon cooling. In **1**$(BF_4)_4$, two of the four iron centers undergo a relatively cooperative one-step SCO, giving rise to a *cis*- rather than *trans*-$(Fe_{HS})_2(Fe_{LS})_2$ isomer,[3] contrary to what was intuitively expected. Surprisingly, all four iron centers keep the HS state in the PF_6^- salt.[3] In **2**-$(CF_3SO_3)_4$, only one iron center adopts the LS state at low temperatures.[4] The origin of such a marked difference in behavior of these closely related compounds has not yet been understood.

Recently, we performed a theoretical study[6] of cyanide-bridged iron(II) square complexes, in which polydentate nitrogen-containing ligands complete the coordination spheres of the iron centers.[7] Although being tetranuclear, these species contain only two SCO centers (the FeN_6 sites, diagonal to each other) and can be considered as a particular case of binuclear SCO complexes. The latter have been studied most intensively among other polynuclear SCO species.[1d,h,j,8−16] These complexes can exist in three spin states, namely, [HS−HS], [HS−LS], and [LS−LS]. As a result, they exhibit different types of thermal SCO. One of them is an usual one-step SCO, [HS−HS] → [LS−LS]. Two other types of spin transition directly involve the

Received: August 4, 2011
Published: October 13, 2011

Scheme 1

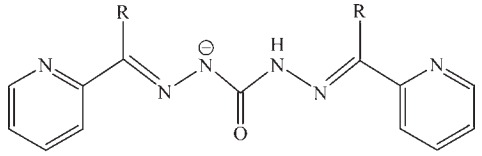

HL^{R-}: R = Ph (**1**)
R = Me (**2**)

mixed-spin state: a partial (50%) SCO, [HS−HS] → [HS−LS], can take place or the transition can occur in two steps, [HS−HS] → [HS−LS] → [LS−LS]. The thermodynamical model[8] demonstrated that the [HS−LS] state enthalpy must be lower than the halfway point between the enthalpies of the [LS−LS] and [HS−HS] states to have a two-step spin transition. The density functional theory (DFT) calculations carried out for a series of binuclear complexes demonstrated the validity of this energetic criterion for two-step SCO.[17] DFT analysis of cyanide-bridged iron(II) squares demonstrated that for all complexes of the series the structurally optimized mixed-spin state lies about in the middle of the energy gap between the structurally optimized homogeneous spin states, thereby satisfying the conditions for a one-step SCO between [LS−LS] and [HS−HS].[6] It was proposed by Matouzenko et al.[16] that stabilization of the intermediate [HS−LS] state in binuclear complexes, and thus the nature of SCO, is due to distortion of the geometry around the HS center induced by SCO on the neighbor and conditioned by the strain effects in bridging and terminal ligands. Analysis of the optimized structures of cyanide-bridged iron(II) squares revealed that the distortion caused by SCO on one transiting center is fully absorbed by the LS FeN_4C_2 sites.[6]

The situation is much more complex in [2 × 2] grid-type species. All four transiting centers are interlocked by extended ligands and communicate through electronic and elastic interactions. In the present paper, we performed the quantum-chemical analysis to elucidate the features of the magnetic behavior of the **1**- and **2**-based compounds. To that end, we characterized structurally (through geometry optimization) and energetically possible spin states of **1** and **2**. Because the calculations concern molecules in the gas phase, they allow one to separate the effects inherent to isolated molecules and those resulting from the crystal environment, and thus they provide a useful tool to detect the intramolecular factors influencing the SCO process. The previous studies[16,17] have demonstrated that quantum-chemical calculations provide adequate structural information for all spin states and are capable of describing the energetics of binuclear SCO complexes. The Continuous Shape Measures (CShM) method[18,19] was further applied to characterize the evolution of coordination polyhedra of iron centers in the optimized and available crystal structures. By means of the CShM, one can analyze the structural response of each center to a spin conversion on any of its neighbors. We also evaluated the strength of exchange interactions effective in spin states with more than one paramagnetic center to estimate the impact of the exchange coupling on the SCO behavior for the given iron(II) grids.

THEORETICAL DETAILS

Calculations reported in this paper were performed within the DFT framework using the *PRIRODA*[20,21] (version 5.0[22]) and *GAUSSIAN09*[23] packages. Different all-electron GTO basis sets were used, namely, the so-called 3z[24] (of TZ2P quality) and L2[25] (compatible with cc-pVTZ) basis sets implemented in the *PRIRODA* package, whereas the *GAUSSIAN09* calculations were carried out using the TZVP basis set reported by Ahlrichs and co-workers.[26]

Geometry Optimizations and Single-Point Energy Calculations. The choice of the better-suited exchange-correlation functional for the description of SCO complexes has been widely debated in the literature,[27] and a complete consensus has not yet been achieved. In the present study, we adopted the computational procedure proven to be the best-performing for a series of cyanide-bridged iron(II) squares; namely, calculations were carried out within the Perdew−Burke−Ernzerhof (PBE)[28,29] framework (PBE/3z for geometry optimizations and PBE/L2 for single-point energy calculations). Although the PBE method overestimates the energy gaps between the neighboring spin states [$(Fe_{HS})_4$ and $(Fe_{HS})_3(Fe_{LS})_1$, $(Fe_{HS})_3(Fe_{LS})_1$ and $(Fe_{HS})_2(Fe_{LS})_2$, etc.], the resulting ΔE values are expected to incorporate approximately the same amount of error and therefore allow one to draw conclusions based on the relative energies of the $(Fe_{HS})_n(Fe_{LS})_{4-n}$ states. For any state with more than one HS iron center, where the exchange coupling can generate a series of spin multiplets, we considered the state with the highest total spin (the only state represented by a single-determinant wave function), supposing that the structure is not very sensitive to the total spin value when local spins are fixed. In all cases, the spin densities at the iron centers were found to be about 0 and 3.7 for local spins equal to 0 and 2, respectively.

Exchange Coupling. The strength of exchange interactions effective in spin states with more than one HS iron center was evaluated for optimized and crystal structures using the broken symmetry (BS) methodology. All possible single determinants (HS and BS) were computed within the framework of the UB3LYP/TZVP computational procedure whose reliability has been repeatedly established.[30,31] The computed $\langle \mathbf{S}^2 \rangle_{HS}$ and $\langle \mathbf{S}^2 \rangle_{BS}$ values are close to those expected for the corresponding spin states; in all cases, the deviations are no more than 0.16. The schemes proposed by Noodleman and co-workers,[32] Ruiz and co-workers,[30] and Yamaguchi and co-workers[33] were used. In the case of two interacting centers, the corresponding equations are given in ref 6. For the $(Fe_{HS})_4$ state, the differences in energy between the HS state and each of the seven BS states were expressed as linear functions of J_{ij} and solved by a least-squares fitting procedure. The J_{ij} values reported in this paper correspond to the following expression of the Heisenberg−Dirac−van Vleck spin Hamiltonian:

$$\mathbf{H} = -\sum_{ij} J_{ij}\mathbf{S}_i\mathbf{S}_j$$

CShM. The concept of CShM was introduced to characterize a relative deviation of different coordination polyhedra from ideal polyhedra described by a particular point symmetry group.[18] It is well-known that for mononuclear iron(II) SCO complexes with a FeN_6 coordination core the LS structures are more regular, i.e., more close to an ideal octahedron. It is quite understandable for the state with a quasi-closed-shell electronic configuration. In contrast, the HS state is characterized by a more irregular structure. An open-shell electronic configuration may lead to a vibronic pseudo-Jahn−Teller-type mixing of different states through nonsymmetric distortions. Thus, the HS state can be

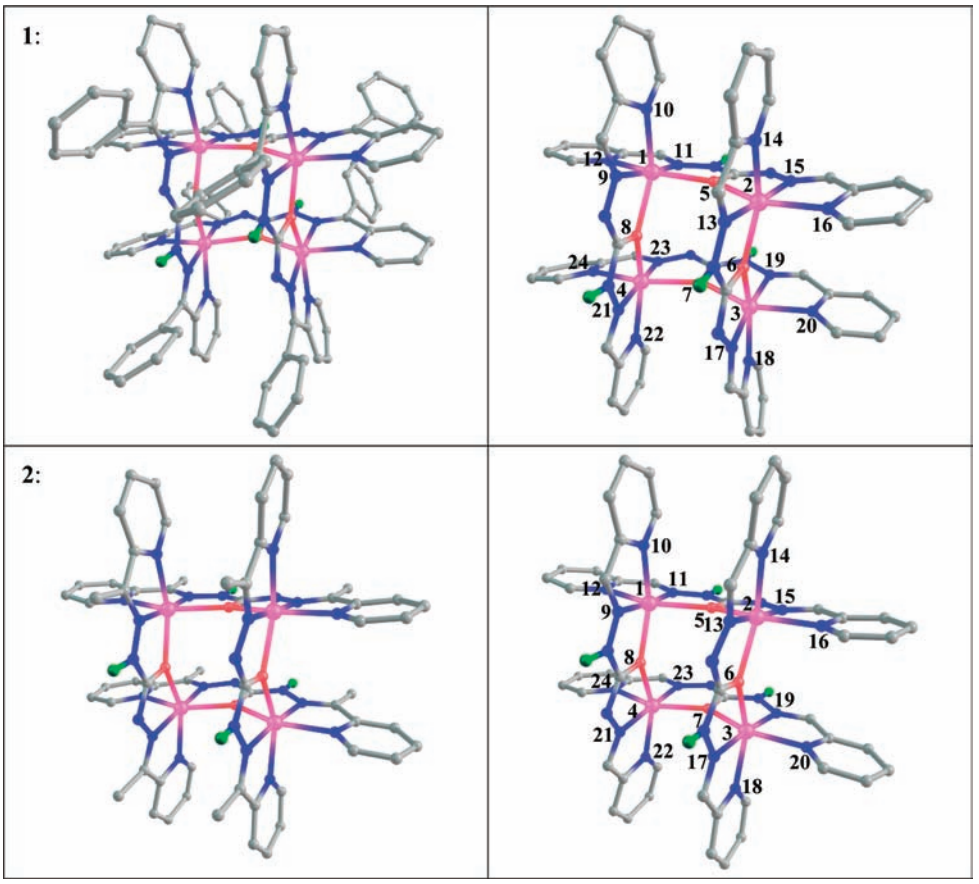

Figure 1. Molecular and core structures of **1** and **2** (optimized structures in the [HS−HS−HS−HS] state are presented). Iron, nitrogen, oxygen, carbon, and hydrogen atoms are shown in pink, blue, red, gray, and green, respectively.

obtained from the LS-state ideal octahedron not only through the totally symmetric dilatation of the coordination sphere but also through other types of distortions lowering the symmetry.[19] Of course, the coordination polyhedron for complexes with the FeN_4O_2 core must deviate from an ideal octahedron in any state, but one can suppose (and it is confirmed by the DFT calculations presented below) that it is more regular and thus closer to the ideal shape in the LS state.

Mathematically, CShM of the coordination polyhedron Q with the geometric center $\vec{q}_0$ relative to an ideal polyhedron P is expressed as

$$S_Q(P) = \min\left[\frac{\sum_{i=1}^{N} |\vec{q}_i - \vec{p}_i|^2}{\sum_{i=1}^{N} |\vec{q}_i - \vec{q}_0|^2}\right] \times 100$$

where $\vec{q}_i$ and $\vec{p}_i$ are the position vectors for atoms of two polyhedra. Both nitrogen and oxygen donor atoms are included, and CShM relative to an ideal octahedron (octahedricity) is calculated using the *SHAPE* program.[34]

RESULTS AND DISCUSSION

Before discussing the results of calculations, we note an important difference in the bridging network in **1** and **2**. These complexes differ not only in the substituent in the interlocking ligand (phenyl for **1** and methyl for **2**) but also in the relative positions of the hydrogen atoms in the bridging network. The close inspection of the N−N and N−C distances in the carbohydrazide skeleton, N−N−C(O)−N−N, in the available X-ray structures of **1** (283 and 123 K) and **2** (123 K) allows one to assign the position of the hydrogen atom: the closeness of the N−N and N−C distances is indicative of the presence of a hydrogen atom at the central nitrogen atom, whereas the hydrogen-free nitrogen atom forms relatively long (N−N) and short (N−C) bonds (Δd = ∼0.08 Å). In addition, the N−N(H)−C bond angle (∼114°) is larger compared to the N−N−C one (∼108°). It appears that in **1** each iron center has both the hydrogen-containing and hydrogen-free five-membered bridging fragments, whereas in **2** the two iron centers on the diagonal of the square have solely hydrogen-containing bridging fragments and the other two hydrogen-free ones. The molecular structures of **1** and **2**, along with their core structures, are shown in Figure 1.

Selected bond lengths for the optimized structures of **1** and **2** in different spin states are collected in Tables 1 and 2. It is worth noting that the optimized structure approximates the equilibrium configuration of the isolated complex in a given spin state, whereas the X-ray structure not only includes the distortions induced by the crystal lattice but also may not correspond to the pure spin state. Nevertheless, for comparison, for the spin states that are close to those characterized by X-ray crystallography, we give the available experimental data in parentheses. It can be seen that the optimized structural parameters are in good agreement with the experimentally found values, with the exception of the Fe−O bond lengths. Let us also note that the tetranuclear core is

dx.doi.org/10.1021/ic2016929 |*Inorg. Chem.* 2011, 50, 11143–11151

Table 1. Selected Bond Lengths (Å) in Optimized and Experimental Structures of 1 in Different Spin States[a]

	$(Fe_{LS})_4$	$(Fe_{HS})_1(Fe_{LS})_3$	*cis*-$(Fe_{HS})_2(Fe_{LS})_2$	*trans*-$(Fe_{HS})_2(Fe_{LS})_2$	$(Fe_{HS})_3(Fe_{LS})_1$	$(Fe_{HS})_4$
Fe_1-N_9	1.88	2.07	2.08 (2.10)[b]	2.06	2.08	2.09 (2.10)[c]
Fe_1-N_{10}	1.95	2.17	2.17 (2.20)	2.17	2.17	2.17 (2.20)
Fe_1-N_{11}	1.89	2.09	2.10 (2.12)	2.08	2.10	2.11 (2.14)
Fe_1-N_{12}	1.95	2.16	2.16 (2.17)	2.17	2.16	2.16 (2.20)
Fe_1-O_5	2.10	2.22	2.18 (2.10)	2.22	2.17	2.16 (2.12)
Fe_1-O_8	2.10	2.25	2.28 (2.14)	2.24	2.28	2.25 (2.14)
Fe_2-N_{13}	1.89	1.89	2.10 (2.11)	1.89	2.11	2.11 (2.13)
Fe_2-N_{14}	1.95	1.95	2.17 (2.13)	1.95	2.16	2.16 (2.17)
Fe_2-N_{15}	1.88	1.89	2.09 (2.07)	1.89	2.10	2.09 (2.10)
Fe_2-N_{16}	1.95	1.95	2.17 (2.16)	1.95	2.17	2.17 (2.21)
Fe_2-O_5	2.10	2.07	2.22 (2.10)	2.09	2.25	2.25 (2.12)
Fe_2-O_6	2.10	2.11	2.21 (2.08)	2.08	2.17	2.16 (2.08)
Fe_3-N_{17}	1.88	1.88	1.89 (1.96)	2.06	2.08	2.09 (2.11)
Fe_3-N_{18}	1.95	1.95	1.95 (2.03)	2.17	2.17	2.17 (2.17)
Fe_3-N_{19}	1.89	1.89	1.89 (1.91)	2.08	2.10	2.11 (2.13)
Fe_3-N_{20}	1.95	1.95	1.95 (2.00)	2.17	2.17	2.16 (2.14)
Fe_3-O_7	2.10	2.10	2.10 (2.01)	2.22	2.20	2.16 (2.08)
Fe_3-O_6	2.10	2.09	2.06 (2.05)	2.24	2.22	2.25 (2.14)
Fe_4-N_{21}	1.89	1.89	1.89 (1.97)	1.89	1.89	2.11 (2.14)
Fe_4-N_{22}	1.95	1.95	1.95 (2.05)	1.95	1.95	2.16 (2.19)
Fe_4-N_{23}	1.88	1.89	1.88 (1.95)	1.89	1.89	2.09 (2.11)
Fe_4-N_{24}	1.95	1.95	1.95 (2.02)	1.95	1.95	2.17 (2.16)
Fe_4-O_7	2.10	2.12	2.11 (2.05)	2.09	2.08	2.25 (2.12)
Fe_4-O_8	2.10	2.07	2.06 (2.05)	2.08	2.07	2.16 (2.11)

[a] Available X-ray structural data are given in parentheses. [b] X-ray structural data collected for $\mathbf{1}(BF_4)_4$ at 123 K (ref 3). [c] X-ray structural data collected for $\mathbf{1}(BF_4)_4$ at 283 K (ref 3).

more compact in the crystal structure compared to the optimized one (the difference in the Fe···Fe distances is about 0.3 Å). Thus, smaller Fe−O bond lengths found in the crystal structures may be a consequence of the crystal-packing effects. Tables 3 and 4 contain the octahedricity values characterizing the distortion of the FeN_4O_2 coordination cores in the optimized and available crystal structures of **1** and **2**. We can note that an integral characteristic, such as CShM, attenuates the differences found between the experimental and calculated bond lengths.

Let us first analyze the structural and energetic behavior of **1**. From Tables 1 and 3, it can be seen that, in the $(Fe_{HS})_4$ state, the iron centers have highly distorted geometries, which deviate essentially from an octahedral symmetry. In the optimized structure, where the coordination polyhedra of iron centers are equivalent, all bond angles deviate from 90 or 180°, particularly the N_p-Fe-O bond angles (the average is 148.6°); see Figure 2a. Interestingly, there is an asymmetry in the Fe−O bond lengths (the Fe−O bond is shorter in the hydrogen-containing five-membered ring). The grid itself adopts a bent conformation with a dihedral angle of 161.9°; the iron centers are separated by 4.09 Å; the Fe−O−Fe bond angles are 136.3°.

The HS → LS transition on one center gives rise to a $(Fe_{HS})_3(Fe_{LS})_1$ species. Irrespective of the site chosen as a target for spin transition, the coordination polyhedra of the corresponding iron centers are equivalent in the resulting structures, and therefore all of the $(Fe_{HS})_3(Fe_{LS})_1$ isomers are energetically degenerate. From Table 1, it can be seen that SCO on the Fe(4) center results in contraction of the Fe−L bonds. The bond angles become more regular; for example, the average N_p-Fe-O bond angle increases to 161.1° (see Figure 2b). It is evident that the LS Fe(4) polyhedron in the [HS−HS−HS−LS] structure is closer to an octahedral configuration (the octahedricity value decreases to 2.02). It should be noted that the majority of mononuclear iron(II) SCO complexes with a FeN_6 coordination core in the LS state are characterized by octahedricity values close to zero (see the Theoretical Details section). The HS → LS reorganization of the Fe(4) coordination sphere affects the geometries around all other centers. For example, the Fe(1) and Fe(3) centers, which are neighboring Fe(4), have smaller octahedricity values [5.07 and 5.04 compared to 5.16 in the $(Fe_{HS})_4$ state]. Interestingly, the asymmetry in the Fe(1)−O bond lengths becomes more pronounced compared to the $(Fe_{HS})_4$ structure, whereas it is almost absent for the Fe(3) center. Thus, the latter has a smaller octahedricity value (5.04). As for the Fe(2) center, which is diagonal to Fe(4), it adopts a more distorted geometry, and the octahedricity value increases to 5.33. The other mixed-spin species contain two or three LS centers, i.e., *cis*- or *trans*-$(Fe_{HS})_2(Fe_{LS})_2$ and $(Fe_{HS})_1(Fe_{LS})_3$. For any of the three cases, the coordination polyhedra of the corresponding iron centers are equivalent in the isomeric forms, and the latter are energetically degenerate. Without going into detail, our calculations confirm that SCO on a given iron center affects the geometries around all others (see Tables 1 and 3).

In the $(Fe_{LS})_4$ state, the Fe−L bond lengths fall in the range typical for LS iron(II) centers, all of the Fe−O bond lengths become equal, the Fe···Fe distances are slightly smaller (4.01 Å), and the Fe−O−Fe bond angles are larger (145.4°) compared to the $(Fe_{HS})_4$ state, but the grid retains a bent conformation

dx.doi.org/10.1021/ic2016929 |*Inorg. Chem.* 2011, 50, 11143–11151

Table 2. Selected Bond Lengths (Å) in Optimized and Experimental Structures of 2 in Different Spin States[a]

	$(Fe_{LS})_4$	$(Fe_{HS})_1(Fe_{LS})_3$		*cis*-$(Fe_{HS})_2(Fe_{LS})_2$	*trans*-$(Fe_{HS})_2(Fe_{LS})_2$		$(Fe_{HS})_3(Fe_{LS})_1$		$(Fe_{HS})_4$
Fe_1-N_9	1.88	1.88	1.88	2.10	2.09	1.88	2.11	2.10 (2.09)[b]	2.12
Fe_1-N_{10}	1.96	1.95	1.96	2.18	2.17	1.95	2.18	2.18 (2.17)	2.18
Fe_1-N_{11}	1.88	1.88	1.88	2.11	2.09	1.88	2.11	2.10 (2.09)	2.10
Fe_1-N_{12}	1.96	1.95	1.96	2.17	2.17	1.95	2.18	2.16 (2.15)	2.17
Fe_1-O_5	2.10	2.11	2.09	2.20	2.24	2.07	2.22	2.18 (2.09)	2.17
Fe_1-O_8	2.10	2.06	2.09	2.24	2.24	2.07	2.20	2.29 (2.14)	2.27
Fe_2-N_{13}	1.89	1.89	1.89	2.08	1.89	2.07	2.08	2.09 (2.11)	2.09
Fe_2-N_{14}	1.95	1.95	1.95	2.16	1.95	2.15	2.16	2.16 (2.18)	2.16
Fe_2-N_{15}	1.89	1.89	1.89	2.09	1.89	2.07	2.08	2.10 (2.11)	2.10
Fe_2-N_{16}	1.95	1.95	1.95	2.16	1.95	2.15	2.15	2.17 (2.18)	2.18
Fe_2-O_5	2.12	2.12	2.12	2.24	2.08	2.30	2.24	2.26 (2.13)	2.26
Fe_2-O_6	2.12	2.12	2.07	2.27	2.08	2.30	2.30	2.21 (2.13)	2.19
Fe_3-N_{17}	1.88	1.88	2.10	1.88	2.09	1.88	1.88	2.11 (2.13)	2.12
Fe_3-N_{18}	1.96	1.95	2.18	1.95	2.17	1.95	1.95	2.18 (2.18)	2.18
Fe_3-N_{19}	1.88	1.88	2.10	1.88	2.09	1.88	1.88	2.10 (2.13)	2.10
Fe_3-N_{20}	1.96	1.95	2.18	1.95	2.17	1.95	1.95	2.18 (2.19)	2.17
Fe_3-O_7	2.10	2.06	2.23	2.10	2.24	2.07	2.06	2.20 (2.13)	2.17
Fe_3-O_6	2.10	2.11	2.23	2.06	2.24	2.07	2.06	2.24 (2.11)	2.27
Fe_4-N_{21}	1.89	2.08	1.89	1.89	1.89	2.07	2.09	1.89 (1.90)	2.09
Fe_4-N_{22}	1.95	2.16	1.95	1.95	1.95	2.15	2.16	1.95 (1.97)	2.16
Fe_4-N_{23}	1.89	2.08	1.89	1.89	1.89	2.07	2.08	1.89 (1.89)	2.10
Fe_4-N_{24}	1.95	2.16	1.95	1.95	1.95	2.15	2.16	1.95 (1.97)	2.18
Fe_4-O_7	2.12	2.28	2.07	2.12	2.08	2.30	2.28	2.08 (2.03)	2.26
Fe_4-O_8	2.12	2.28	2.12	2.06	2.08	2.30	2.25	2.07 (2.03)	2.19

[a] Available X-ray structural data are given in parentheses. [b] X-ray structural data collected for $\mathbf{2}(CF_3SO_3)_4$ at 123 K (ref 4).

(a dihedral angle = 162.6°). From Table 3, it can be seen that the coordination polyhedra of iron centers become more distorted (less octahedral) compared to the LS characteristics in the mixed-spin states.

The relative energies for the structurally optimized spin states of **1** (see Table 5) correspond to the behavior expected for SCO systems. The $(Fe_{LS})_4$ state is found to be the ground state. According to calculations, the energies of the $(Fe_{HS})_n(Fe_{LS})_{4-n}$ species increase with the successive appearance of HS sites. Interestingly, among the $(Fe_{HS})_2(Fe_{LS})_2$ species, a *cis* structure proves to be more stable than a trans one, in agreement with the experimentally found feature. If we consider separately the Fe(1)−Fe(2) and Fe(3)−Fe(4) pairs, for each of these pairs, the energy of the [HS−LS] state is close to the halfway point between the energies of the [HS−HS] and [LS−LS] states, thereby favoring a one-step transition. At the same time, the energy of the [HS−HS−LS−LS] state is lower than the halfway point between the energies of the [HS−HS−HS−HS] and [LS−LS−LS−LS] states. If the energetic criterion obtained for binuclear complexes is valid for tetranuclear species, one can say that the conditions are satisfied for stabilization of the [HS−HS−LS−LS] state.

The magnetic behavior of the **1**-based compounds and, in particular, a partial (50%) SCO observed in $\mathbf{1}(BF_4)_4$ can be rationalized on the basis of the data presented above. When discussing the optimized structures of **1**, we pointed out that SCO on one iron center affects the geometries around the others. The structural changes can be monitored and quantified by comparing the octahedricity values. In other words, the core structure, being rigid and compact, does not absorb the distortion caused by SCO and transmits it not only to the neighbors but also to the remote (diagonal) site. This situation differs from that in the cyanide-bridged iron(II) squares, where the two active sites are fully independent. The core structure of **1** imposes steric constraints and thus provides the energetic proximity of the $(Fe_{HS})_n(Fe_{LS})_{4-n}$ states. At the same time, the rigidity of the ligand and grid itself controls the barrier for the spin-state transformation. In **1**, the distortions accompanying the transition to a new spin state are costly in energy because they give rise to highly strained structures. The barrier corresponding to the crossing-point structure can be overcome only at relatively high temperatures. For the isolated complexes, one would expect the following SCO behavior. At room temperature, all four iron centers reside in the HS state. Upon cooling, the HS → LS transition on one center takes place, as both the thermodynamic and kinetic conditions are met, and thus the $(Fe_{HS})_3(Fe_{LS})_1$ species arise. The latter contain the three different HS centers, one of which became less octahedral (5.16 → 5.33), whereas the other two, in the cis positions to the LS center, moved to be more octahedral (5.16 → 5.07 or 5.04), i.e., their coordination polyhedra approach the LS characteristics. The energy gap between the $(Fe_{HS})_3(Fe_{LS})_1$ and *cis*-$(Fe_{HS})_2(Fe_{LS})_2$ states is about the same as that between the $(Fe_{HS})_4$ and $(Fe_{HS})_3(Fe_{LS})_1$ states, and thus SCO on any of these two centers is thermodynamically possible. The two more octahedral HS centers in the $(Fe_{HS})_3(Fe_{LS})_1$ species should have lower barriers for the spin-state transformation, and thus SCO on any of these two centers is facilitated in terms of kinetics. As a result, the weight fraction of the *cis*-$(Fe_{HS})_2(Fe_{LS})_2$ species rapidly increases upon cooling. We highlight the fact that on going from $(Fe_{HS})_4$ to *cis*-$(Fe_{HS})_2(Fe_{LS})_2$

dx.doi.org/10.1021/ic2016929 |*Inorg. Chem.* 2011, 50, 11143–11151

Table 3. Octahedricity Values for Different Iron Centers in Optimized and Experimental Structures of 1

	Fe(1)	Fe(2)	Fe(3)	Fe(4)
$(Fe_{LS})_4$	2.16	2.16	2.16	2.16
$(Fe_{HS})_1(Fe_{LS})_3$	5.07	2.17	2.05	2.15
cis-$(Fe_{HS})_2(Fe_{LS})_2$	5.23 (5.66)[a]	5.20 (5.22)	2.07 (3.18)	2.04 (3.34)
trans-$(Fe_{HS})_2(Fe_{LS})_2$	4.94	2.11	4.94	2.11
$(Fe_{HS})_3(Fe_{LS})_1$	5.07	5.33	5.04	2.02
$(Fe_{HS})_4$	5.15 (5.49)[b]	5.16 (5.56)	5.16 (5.60)	5.16 (5.77)

[a] X-ray structural data collected for $1(BF_4)_4$ at 123 K were used (ref 3). [b] X-ray structural data collected for $1(BF_4)_4$ at 283 K were used (ref 3).

Table 4. Octahedricity Values for Different Iron Centers in Optimized and Experimental Structures of 2

	Fe(1)	Fe(2)	Fe(3)	Fe(4)
[LS−LS−LS−LS]	2.11	2.23	2.12	2.23
[LS−LS−LS−HS]	2.03	2.19	2.03	5.15
[LS−LS−HS−LS]	2.05	2.13	5.43	2.13
[HS−HS−LS−LS]	5.53	5.27	1.96	2.08
[HS−LS−HS−LS]	5.27	2.03	5.28	2.03
[LS−HS−LS−HS]	1.91	5.08	1.90	5.08
[HS−HS−LS−HS]	5.53	5.15	1.84	5.13
[HS−HS−HS−LS]	5.44 (5.09)[a]	5.35 (5.65)	5.34 (5.68)	1.96 (2.34)
[HS−HS−HS−HS]	5.41	5.17	5.41	5.17

[a] X-ray structural data collected for $2(CF_3SO_3)_4$ at 123 K were used (ref 4).

the change of the spin state at one center facilitates SCO on another one. Such an assistance is nothing but a manifestation of the intramolecular cooperativity. The occurrence of the *trans*-$(Fe_{HS})_2(Fe_{LS})_2$ species is scarcely probable. As we mentioned before, in the $(Fe_{HS})_3(Fe_{LS})_1$ species, changes in the coordination polyhedron of the center *trans* to the LS one move it away from the LS characteristics, and thus the barrier for the spin-state transformation should be higher in this case. Let us remind everyone that this transition is also less favorable energetically. In the *cis*-$(Fe_{HS})_2(Fe_{LS})_2$ species, the two HS centers have even more distorted (less octahedral) geometries than in the initial $(Fe_{HS})_4$ state, as evidenced by the octahedricity values (5.23 and 5.20 compared to 5.16). Thus, for either of the two centers, the barrier for the spin-state transformation is even higher than that at the starting point, whereas the temperature is lower. In such circumstances, SCO is kinetically blocked, and the complexes keep the *cis*-$(Fe_{HS})_2(Fe_{LS})_2$ state upon further cooling. As we mentioned in the Introduction, such a behavior is observed in $1(BF_4)_4$. The variable-temperature magnetic susceptibility measurements show a relatively cooperative one-step SCO on two iron centers in this compound. The Mössbauer measurements, in conjunction with X-ray crystallographic analysis, suggest the complete transition of two neighboring iron centers below 120 K. At the same time, $1(PF_6)_4$ does not display a spin transition and thus demonstrates a deviation from the isolated molecule behavior. A possible explanation of this fact is that, in the solid state, the energy gaps between the $(Fe_{HS})_n(Fe_{LS})_{4-n}$ states and the barriers for the spin-state transformation may differ to some extent from those in the isolated complexes because the crystal lattice imposes additional steric constraints. For example, in the X-ray structure of $1(BF_4)_4$ corresponding to the $(Fe_{HS})_4$ phase

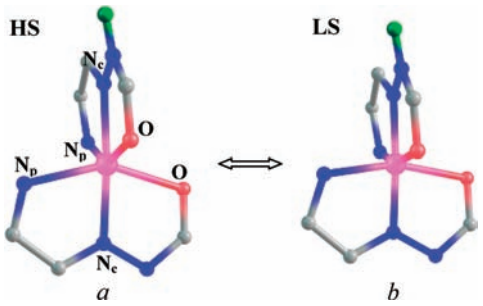

Figure 2. FeN_4O_2 coordination cores in HS (a) and LS (b) states in **1**. N_p and N_c are the donor nitrogen atoms in the pyridine moiety and carbohydrazide skeleton, respectively.

Table 5. Relative Energies of Different Spin-State Isomers of 1 Calculated at the Optimized Geometries (in kJ mol^{-1})

species	ΔE[a]
$(Fe_{LS})_4$	0.0
$(Fe_{HS})_1(Fe_{LS})_3$	57.0
cis-$(Fe_{HS})_2(Fe_{LS})_2$	114.4
trans-$(Fe_{HS})_2(Fe_{LS})_2$	116.6
$(Fe_{HS})_3(Fe_{LS})_1$	175.0
$(Fe_{HS})_4$	235.9

[a] The energy of the $(Fe_{LS})_4$ species is taken as zero.

(283 K), the grid is more compact, and the coordination polyhedra of iron centers are more distorted (less octahedral) compared to those in the optimized $(Fe_{HS})_4$ structure. Importantly, two of the four iron centers are involved in intermolecular $\pi-\pi$ interactions, and thus these two centers apparently have lower barriers for the spin-state transformation because distortion toward the more compact LS geometry reduces the steric strain caused by short intermolecular contacts. As a result, SCO on any of these two centers is kinetically possible and actuates the whole process. The PF_6^- salt apparently has a different crystal packing motif, in which case the barriers for the spin-state transformation cannot be overcome at room temperature. Unfortunately, the X-ray data for this compound were not reported.

Before completing this part of the discussion, we consider the effect of exchange coupling in **1**. The values of J_{ij} for the experimentally observed states, $(Fe_{HS})_4$ and *cis*-$(Fe_{HS})_2(Fe_{LS})_2$, obtained using the algorithm proposed by Yamaguchi et al.,[33] are given in Table 6. The other two schemes mentioned in the Theoretical Details section provide similar results (see Table S1 of the Supporting Information). In all cases, the J_{ij} values indicate a weak antiferromagnetic coupling and explain a smooth decrease of the $\chi_M T$ product upon cooling in the plateau regions corresponding to the $(Fe_{HS})_4$ and *cis*-$(Fe_{HS})_2(Fe_{LS})_2$ phases. The low-temperature behavior is dominated by the zero-field splitting of the local $S = 2$ state in the *cis*-$(Fe_{HS})_2(Fe_{LS})_2$ species. It is worth noting that there is good agreement with the experimental value (-4.5 cm^{-1}) obtained for the *cis*-$(Fe_{HS})_2(Fe_{LS})_2$ state in terms of a simple isotropic model.[3] Although the exchange interactions present an important feature of $[2 \times 2]$ grids, it is not likely that they play an important role in the SCO process. In fact, their energy is rather small compared to the energy gaps between the $(Fe_{HS})_n(Fe_{LS})_{4-n}$ states. The often-mentioned synergy between the exchange coupling and SCO

dx.doi.org/10.1021/ic2016929 |*Inorg. Chem.* 2011, 50, 11143–11151

Table 6. Values of J_{ij} (in cm^{-1}) for Different Spin States Computed for Optimized and Crystal Structures of 1

state	J_{ij}	crystal structure	optimized geometry
cis-$(Fe_{HS})_2(Fe_{LS})_2$	J	−7.3[b]	−5.9
$(Fe_{HS})_4$[a]	J_{12}	−6.25(2)[c]	−5.20(1)
	J_{13}	−0.05(2)	0.00 (1)
	J_{14}	−5.36(2)	−5.20(1)
	J_{23}	−7.88(2)	−5.20(1)
	J_{24}	0.06(2)	0.00(1)
	J_{34}	−3.62(2)	−5.20(1)

[a] The standard errors are given in parentheses. [b] X-ray structural data collected for $\mathbf{1}(BF_4)_4$ at 123 K were used (ref 3). [c] X-ray structural data collected for $\mathbf{1}(BF_4)_4$ at 283 K were used (ref 3).

Table 7. Relative Energies of Different Spin-State Isomers of 2 Calculated at the Optimized Geometries (in kJ mol^{-1})

species	ΔE[a]
[LS−LS−LS−LS]	0.0
[LS−LS−LS−HS]	59.0
[LS−LS−HS−LS]	41.9
[HS−HS−LS−LS]	105.7
[HS−LS−HS−LS]	86.5
[LS−HS−LS−HS]	118.2
[HS−HS−LS−HS]	171.2
[HS−HS−HS−LS]	155.4
[HS−HS−HS−HS]	225.3

[a] The energy of the $(Fe_{LS})_4$ species is taken as zero.

would be more relevant for compounds with comparable characteristic energies. Unfortunately, such compounds have not yet been documented.

Having examined the structural features and the magnetic behavior of **1**, we now discuss how the differences in the molecular structure of **2** may influence the SCO process. As we mentioned before, along with the different substituents at the periphery, **1** and **2** differ in the relative positions of the hydrogen atoms in the bridging network (see Figure 1). It can be seen that in **2** the Fe(1) and Fe(3) centers have solely hydrogen-containing bridging fragments and the Fe(2) and Fe(4) centers hydrogen-free ones. As a result, the mixed-spin species have nonequivalent isomeric forms (see Table 2). Similar to **1**, the stability of the $(Fe_{HS})_n(Fe_{LS})_{4-n}$ species decreases with an increase of the number of HS sites (see Table 7). Interestingly, among a given series (n = 1, 2, or 3), the species with the "hydrogen-containing" HS centers are more stable. In particular, in the case of two HS sites, a cis isomer (one "hydrogen-containing" and one "hydrogen-free" HS center) has an intermediate energy between the energies of the two trans isomers (two "hydrogen-containing" HS centers and two "hydrogen-free" HS centers).

Although the HS and LS polyhedra of iron centers in **2** are similar to those in **1** (see Figure 2a), they have a few important peculiarities. From Tables 2 and 4, it can be seen that, in the optimized $(Fe_{HS})_4$ structure, the "hydrogen-containing" iron centers are less octahedral (5.41) compared to the "hydrogen-free" ones (5.17). Interestingly, the grid itself acquires an asymmetry because for any iron center the Fe···Fe distances (4.11 and 4.14 Å) and the Fe−O−Fe bond angles (136.0 and 136.5°) become different. Although it still adopts a bent conformation, a dihedral angle becomes larger (170.4 compared to 161.9° in **1**). In the optimized $(Fe_{LS})_4$ structure, the "hydrogen-containing" iron centers are more octahedral (2.11 and 2.12) compared to the "hydrogen-free" ones (2.23). For any iron center, the Fe−O bond lengths become equal, but they are smaller at the "hydrogen-containing" centers (2.10 compared to 2.12 Å). The grid itself is flattened (a dihedral angle = 179.2°), all of the Fe···Fe distances are 4.02 Å, and all of the Fe−O−Fe bond angles are 145.1°. Similar to **1**, the structural information presented in Tables 2 and 4 indicates that SCO on one iron center affects the geometries around the others. On the basis of these data, one would expect the following isolated molecule behavior. In the $(Fe_{HS})_4$ state, the "hydrogen-containing" iron centers, being less octahedral, have higher barriers for the spin-state transformation, and thus SCO on any of these two centers is kinetically hindered or even blocked. In contrast, the "hydrogen-free" iron centers have characteristics similar to those for any iron center in **1**, and thus one of them undergoes the HS → LS transition upon cooling. SCO on a "hydrogen-free" iron center is also favored energetically. In the resulting $(Fe_{HS})_3(Fe_{LS})_1$ structure, all three HS centers are less octahedral than the transiting center in the initial $(Fe_{HS})_4$ state and thus have higher barriers for the spin-state transformation. The data in Table 7 suggest that SCO on the second "hydrogen-free" iron center is thermodynamically possible at the same temperature (the energy gap between the [HS−HS−HS−LS] and [HS−LS−HS−LS] states is about the same as that between the [HS−HS−HS−HS] and [HS−HS−HS−LS] states), whereas a *cis*-$(Fe_{HS})_2(Fe_{LS})_2$ state is thermodynamically accessible at lower temperature (the energy gap between the [HS−HS−HS−LS] and [HS−HS−LS−LS] states is smaller); however, obviously SCO on any of the three HS centers in the $(Fe_{HS})_3(Fe_{LS})_1$ species is kinetically blocked. As we mentioned in the Introduction, such a behavior is observed in $\mathbf{2}(CF_3SO_3)_4$. The variable-temperature magnetic susceptibility measurements show a continuous SCO on one iron center in this compound. The X-ray crystallographic data collected at 123 K indicate that the transition occurs on a "hydrogen-free" iron center. Interestingly, in the X-ray structure, one HS center, in a cis position to the LS one, is more octahedral (5.09) compared to the others (5.65 and 5.68). Moreover, it exhibits slightly smaller average Fe−L bond length. These facts may be indicative of the presence of a small admixture of the *cis*-$(Fe_{HS})_2(Fe_{LS})_2$ species in the sample. Indeed, in the solid state, the grid is more compact, and the LS and HS geometries around the iron centers are more distorted because of the crystal-packing effects, and thus the energy gaps between the $(Fe_{HS})_n(Fe_{LS})_{4-n}$ states and the barriers for the spin-state transformation may differ to some extent from those in the isolated complexes. As a result, the occurrence of the *cis*-$(Fe_{HS})_2(Fe_{LS})_2$ species may be feasible at not very low temperatures. Of course, conclusions about the kinetic factors of SCO based on calculated geometrical characteristics are rather qualitative and just give indications in what direction they are shifted on individual centers following the spin transition at neighbors.

It is evident that the SCO behavior of the **1**- and **2**-based compounds is controlled by the rigidity of the ligand and grid itself, and the difference between the two cases is primarily due to the dissimilarity in the core structures, i.e., in the relative positions of the hydrogen atoms in the bridging network. The phenyl rings at the periphery of the ligand in **1** are twisted relative to the ligand plane and do not cause any additional intramolecular strain (see Figure 1).

dx.doi.org/10.1021/ic2016929 |*Inorg. Chem.* 2011, 50, 11143–11151

However, the presence of bulky substituents predetermines the crystal-packing motif. For example, $\mathbf{1}(BF_4)_4$ has a one-dimensional network of intermolecular interactions, whereas $\mathbf{2}(CF_3SO_3)_4$ has a two-dimensional one. Interestingly, variable-temperature magnetic susceptibility measurements revealed a weak cooperativity in $\mathbf{2}$-$(CF_3SO_3)_4$, despite the presence of a two-dimensional network of intermolecular contacts. This fact lends additional support to the conclusion that the cooperativity observed in $\mathbf{1}(BF_4)_4$ is governed by intramolecular factors.

Finally, it is worth noting that a less strained grid comprising a more flexible thiocarbohydrazide-based ligand is diamagnetic in the temperature range 2−300 K.[4] The X-ray crystallographic data collected at 133 K demonstrate that such a ligand is bent along the C−S axis (the average Fe−S−C−Fe dihedral angle = 142.7°). Thus, the core structure, being more flexible and less compact, does not provide the energetic proximity of the $(Fe_{HS})_n(Fe_{LS})_{4-n}$ states.

CONCLUSIONS

Our calculations clearly demonstrate that the SCO behavior of the grid-type complexes is highly determined by the rigidity of the ligands interlocking the metal sites. The rigidity or flexibility of the ligands defines the elastic communication between the transiting centers. These links are spread not only between the neighboring centers but over the whole cluster. Such behavior of $[2 \times 2]$ grids differentiates them from the earlier studied cyanide-bridged squares, where the intermediate FeN_4C_2 sites absorb the corresponding distortion. Small perturbations (such as different positions of the hydrogen atoms in the bridging network) influencing the rigidity of the grid can drastically change the nature of SCO. Analysis of the relative energies of the spin states is not as helpful in predicting the SCO behavior as used to be for binuclear complexes. The evolution of coordination polyhedra accompanying SCO becomes an important indicator related to the kinetic factors of spin-state transformation.

ASSOCIATED CONTENT

Supporting Information. Table containing the J_{ij} values for different spin states computed for optimized and crystal structures of **1**. This material is available free of charge via the Internet at http://pubs.acs.org.

AUTHOR INFORMATION

Corresponding Author

*E-mail: borchtch@ens-lyon.fr (S.A.B.), zueva_ekaterina@mail.ru (E.M.Z.).

REFERENCES

(1) (a) Spin Crossover in Transition Metal Compounds. In *Topics in Current Chemistry*; Gütlich, P., Goodwin, H. A., Eds.; Springer-Verlag: Berlin, 2004; pp 233−235. (b) Bousseksou, A.; Molnár, G.; Matouzenko, G. S. *Eur. J. Inorg. Chem.* **2004**, 4353. (c) Gütlich, P.; Koningsbruggen, P. J. v.; Renz, F. *Struct. Bonding (Berlin)* **2004**, *107*, 27. (d) Gaspar, A. B.; Ksenofontov, V.; Serednyuk, M.; Gütlich, P. *Coord. Chem. Rev.* **2005**, *249*, 2661. (e) Real, J. A.; Gaspar, A. B.; Muñoz, M. C. *Dalton Trans.* **2005**, 2062. (f) Gaspar, A. B.; Muñoz, M. C.; Real, J. A. *J. Mater. Chem.* **2006**, *16*, 2522. (g) Sorai, M.; Nakano, M.; Miyazaki, Y. *Chem. Rev.* **2006**, *106*, 976. (h) Bousseksou, A.; Molnár, G.; Real, J. A.; Tanaka, K. *Coord. Chem. Rev.* **2007**, *251*, 1822. (i) Halcrow, M. A. *Polyhedron* **2007**, *26*, 3523. (j) Murray, K. S. *Eur. J. Inorg. Chem.* **2008**, 3101.

(2) (a) Breuning, E.; Ruben, M.; Lehn, J. M.; Renz, F.; Garcia, Y.; Ksenofontov, V.; Gütlich, P.; Wegelius, E.; Rissanen, K. *Angew. Chem., Int. Ed.* **2000**, *39*, 2504. (b) Ruben, M.; Breuning, E.; Lehn, J. M.; Ksenofontov, V.; Renz, F.; Gütlich, P.; Vaughan, G. B. M. *Chem.—Eur. J.* **2003**, *9*, 4422. (c) Ruben, M.; Ziener, U.; Lehn, J. M.; Ksenofontov, V.; Gütlich, P.; Vaughan, G. B. M. *Chem.—Eur. J.* **2005**, *11*, 94.

(3) Wu, D.-Y.; Sato, O.; Einaga, Y.; Duan, C.-Y. *Angew. Chem., Int. Ed.* **2009**, *48*, 1475.

(4) Shuvaev, K. V.; Dawe, L. N.; Thompson, L. K. *Dalton Trans.* **2010**, 4768.

(5) Schneider, B.; Demeshko, S.; Dechert, S.; Meyer, F. *Angew. Chem., Int. Ed.* **2010**, *49*, 9274.

(6) Zueva, E. M.; Ryabikh, E. R.; Kuznetsov, An. M.; Borshch, S. A. *Inorg. Chem.* **2011**, *50*, 1905.

(7) (a) Oshio, H.; Onodera, H.; Tamada, O.; Mizutani, H.; Hikichi, T.; Ito, T. *Chem.—Eur. J.* **2000**, *6*, 2523. (b) Flay, M.-L.; Comte, V.; Vahrenkamp, H. *Z. Anorg. Allg. Chem.* **2003**, *629*, 1147. (c) Nihei, M.; Ui, M.; Yokota, M.; Han, L.; Maeda, A.; Kishida, H.; Okamoto, H.; Oshio, H. *Angew. Chem., Int. Ed.* **2005**, *44*, 6484. (d) Boldog, I.; Muñoz-Lara, F. J.; Gaspar, A. B.; Muñoz, M. C.; Seredyuk, M.; Real, J. A. *Inorg. Chem.* **2009**, *48*, 3710. (e) Nihei, M.; Ui, M.; Oshio, H. *Polyhedron* **2009**, *28*, 1718.

(8) Real, J. A.; Bolvin, H.; Bousseksou, A.; Dworkin, A.; Kahn, O.; Varret, F.; Zarembowitch, J. *J. Am. Chem. Soc.* **1992**, *114*, 4650.

(9) Real, J. A.; Gaspar, A. B.; Muñoz, M. C.; Gütlich, P.; Ksenofontov, V.; Spiering, H. *Top. Curr. Chem.* **2004**, *233*, 167.

(10) Murray, K. S.; Kepert, C. J. *Top. Curr. Chem.* **2004**, *233*, 195.

(11) (a) Suemura, N.; Ohama, M.; Kaizaki, S. *Chem. Commun.* **2001**, 1538. (b) Nakano, K.; Suemura, N.; Kawata, S.; Fuyuhiro, A.; Yagi, T.; Nasu, S.; Morimoto, S.; Kaizaki, S. *Dalton Trans.* **2004**, 982. (c) Nakano, K.; Kawata, S.; Yoneda, K.; Fuyuhiro, A.; Yagi, T.; Nasu, S.; Morimoto, S.; Kaizaki, S. *Chem. Commun.* **2004**, 2892. (d) Nakano, K.; Suemura, N.; Yoneda, K.; Kawata, S.; Kaizaki, S. *Dalton Trans.* **2005**, 740. (e) Yoneda, K.; Adachi, K.; Hayami, S.; Maeda, Y.; Katada, M.; Fuyuhiro, A.; Kawata, S.; Kaizaki, S. *Chem. Commun.* **2006**, 45.

(12) Létard, J.-F.; Carbonera, C.; Real, J. A.; Kawata, S.; Kaizaki, S. *Chem.—Eur. J.* **2009**, *15*, 4146.

(13) Schneider, C. J.; Cashion, J. D.; Moubaraki, B.; Neville, S. M.; Batten, S. R.; Turner, D. R.; Murray, K. S. *Polyhedron* **2007**, *26*, 1764.

(14) Fedaoui, D.; Bouhadja, Y.; Kaiba, A.; Guionneau, P.; Létard, J.-F.; Rosa, P. *Eur. J. Inorg. Chem.* **2008**, 1022.

(15) Ortega-Villar, N.; Thompson, A. L.; Muñoz, M. C.; Ugalde-Saldívar, V. M.; Goeta, A. E.; Morena-Esparza, R.; Real, J. A. *Chem.—Eur. J.* **2005**, *11*, 5721.

(16) (a) Verat, A. Yu.; Ould-Moussa, N.; Jeanneau, E.; Le Guennic, B.; Bousseksou, A.; Borshch, S. A.; Matouzenko, G. S. *Chem.—Eur. J.* **2009**, *15*, 10070. (b) Matouzenko, G. S.; Jeanneau, E.; Verat, A. Yu.; Bousseksou, A. *Dalton Trans.* **2011**, *40*, 9608.

(17) Zein, S.; Borshch, S. A. *J. Am. Chem. Soc.* **2005**, *127*, 16197.

(18) (a) Avnir, D.; Katzenelson, O.; Keinan, S.; Pinsky, M.; Pinto, Y.; Salomon, Y.; Zabrodsky Hel-Or, H. In *Concepts in Chemistry: A Contemporary Challenge*; Rouvray, D. H., Ed.; Research Studies Press Ltd.: Taunton, England, 1997; Chapter 9, pp 283−324. (b) Zabrodsky, H.; Peleg, S.; Avnir, D. *J. Am. Chem. Soc.* **1992**, *114*, 7843. (c) Alvarez, S.; Avnir, D.; Llunell, M.; Pinsky, M. *New J. Chem.* **2002**, *26*, 996. (d) Alvarez, S.; Alemany, P.; Casanova, D.; Cirera, J.; Llunell, M.; Avnir, D. *Coord. Chem. Rev.* **2005**, *249*, 1693.

(19) Alvarez, S. *J. Am. Chem. Soc.* **2003**, *125*, 6795.

(20) Laikov, D. N. *Chem. Phys. Lett.* **1997**, *281*, 151.

(21) Laikov, D. N.; Ustynyuk, Y. A. *Russ. Chem. Bull., Int. Ed.* **2005**, *54*, 820.

(22) Laikov, D. N. *PRIRODA, Electronic Structure Code*, version 5; 2005.

(23) Frisch, M. J.; Trucks, G. W.; Schlegel, H. B.; Scuseria, G. E.; Robb, M. A.; Cheeseman, J. R.; Scalmani, G.; Barone, V.; Mennucci, B.; Petersson, G. A.; Nakatsuji, H.; Caricato, M.; Li, X.; Hratchian, H. P.; Izmaylov, A. F.; Bloino, J.; Zheng, G.; Sonnenberg, J. L.; Hada, M.; Ehara, M.; Toyota, K.; Fukuda, R.; Hasegawa, J.; Ishida, M.; Nakajima, T.; Honda, Y.; Kitao, O.; Nakai, H.; Vreven, T.; Montgomery, J. A., Jr.;

Peralta, J. E.; Ogliaro, F.; Bearpark, M.; Heyd, J. J.; Brothers, E.; Kudin, K. N.; Staroverov, V. N.; Kobayashi, R.; Normand, J.; Raghavachari, K.; Rendell, A.; Burant, J. C.; Iyengar, S. S.; Tomasi, J.; Cossi, M.; Rega, N.; Millam, J. M.; Klene, M.; Knox, J. E.; Cross, J. B.; Bakken, V.; Adamo, C.; Jaramillo, J.; Gomperts, R.; Stratmann, R. E.; Yazyev, O.; Austin, A. J.; Cammi, R.; Pomelli, C.; Ochterski, J.; Martin, R. L.; Morokuma, K.; Zakrzewski, V. G.; Voth, G. A.; Salvador, P.; Dannenberg, J. J.; Dapprich, S.; Daniels, A. D.; Farkas, O.; Foresman, J. B.; Ortiz, J. V.; Cioslowski, J.; Fox, D. J. *GAUSSIAN09*, revision A.02; Gaussian, Inc.: Wallingford, CT, 2009.

(24) Laikov, D. N. Ph.D. Thesis, Moscow State University, Moscow, 2000.

(25) Laikov, D. N. *Chem. Phys. Lett.* **2005**, *416*, 116.

(26) Schafer, A.; Horn, H.; Ahlrichs, R. *J. Chem. Phys.* **1994**, *100*, 5829.

(27) (a) Reiher, M. *Inorg. Chem.* **2002**, *41*, 6928. (b) Paulsen, H.; Trautwein, A. X. *Top. Curr. Chem.* **2004**, *235*, 197. (c) Fouqueau, A.; Mer, S.; Casida, M. E.; Daku, L. M. L.; Hauser, A.; Mineva, T.; Neese, F. *J. Chem. Phys.* **2004**, *120*, 9473. (d) Fouqueau, A.; Casida, M. E.; Daku, L. M. L.; Hauser, A.; Neese, F. *J. Chem. Phys.* **2005**, *122*, 044110. (e) Daku, L. M. L.; Vargas, A.; Hauser, A.; Fouqueau, A.; Casida, M. E. *ChemPhysChem* **2005**, *6*, 1393. (f) Ganzenmüller, G.; Berkaïne, N.; Fouqueau, A.; Casida, M. E.; Reiher, M. J. *Chem. Phys.* **2005**, *122*, 234321. (g) Pierloot, K.; Vancoillie, S. *J. Chem. Phys.* **2006**, *125*, 124303. (h) Zein, S.; Borshch, S. A.; Fleurat-Lessard, P.; Casida, M. E.; Chermette, H. *J. Chem. Phys.* **2007**, *126*, 014105. (i) Pierloot, K.; Vancoillie, S. *J. Chem. Phys.* **2008**, *128*, 034104. (j) Swart, M. *J. Chem. Theory Comput.* **2008**, *4*, 2057. (k) Güell, M.; Luis, J. M.; Solà, M.; Swart, M. *J. Phys. Chem. A* **2008**, *112*, 6384. (l) Jensen, K. P.; Cirera, J. *J. Phys. Chem. A* **2009**, *113*, 10033. (m) Ye, S.; Neese, F. *Inorg. Chem.* **2010**, *49*, 772.

(28) Perdew, J. P.; Burke, K.; Ernzerhof, M. *Phys. Rev. Lett.* **1996**, *77*, 3865.

(29) Perdew, J. P.; Burke, K.; Ernzerhof, M. *Phys. Rev. Lett.* **1997**, *78*, 1396.

(30) (a) Ruiz, E.; Cano, J.; Alvarez, S.; Alemany, P. *J. Comput. Chem.* **1999**, *20*, 1391. (b) Ruiz, E.; Rodriguez-Fortea, A.; Cano, J.; Alvarez, S.; Alemany, P. *J. Comput. Chem.* **2003**, *24*, 982. (c) Ruiz, E.; Alvarez, S.; Cano, J.; Polo, V. *J. Chem. Phys.* **2005**, *123*, 164110.

(31) (a) Ruiz, E.; Alemany, P.; Alvarez, S.; Cano, J. *J. Am. Chem. Soc.* **1997**, *119*, 1297. (b) Ruiz, E.; Alemany, P.; Alvarez, S.; Cano, J. *Inorg. Chem.* **1997**, *36*, 3683. (c) Ruiz, E.; Cano, J.; Alvarez, S.; Alemany, P. *J. Am. Chem. Soc.* **1998**, *120*, 11122. (d) Ruiz, E.; Rodriguez-Fortea, A.; Alemany, P.; Alvarez, S. *Polyhedron* **2001**, *20*, 1323. (e) Ruiz, E.; Graaf, C.; Alemany, P.; Alvarez, S. *J. Phys. Chem. A* **2002**, *106*, 4938. (f) Ruiz, E.; Cano, J.; Alvarez, S.; Caneschi, A.; Gatteschi, D. *J. Am. Chem. Soc.* **2003**, *125*, 6791. (g) Ghosh, P.; Bill, E.; Weyhermuller, T.; Neese, F.; Wieghardt, K. *J. Am. Chem. Soc.* **2003**, *125*, 1293. (h) Rodriguez-Fortea, A.; Alemany, P.; Alvarez, S.; Ruiz, E. *Eur. J. Inorg. Chem.* **2004**, 143. (i) Cano, J.; Costa, R.; Alvarez, S.; Ruiz, E. *J. Chem. Theory Comput.* **2007**, *3*, 782. (j) Zueva, E. M.; Borshch, S. A.; Petrova, M. M.; Chermette, H.; Kuznetsov, An. M. *Eur. J. Inorg. Chem.* **2007**, *27*, 4317. (k) Aronica, C.; Chastanet, G.; Zueva, E. M.; Borshch, S. A.; Clemente-Juan, J. M.; Luneau, D. *J. Am. Chem. Soc.* **2008**, *130*, 2365. (l) Zueva, E. M.; Petrova, M. M.; Herchel, R.; Trávníček, Z.; Raptis, R.; Mathivathanan, L.; McGrady, J. E. *Dalton Trans.* **2009**, *30*, 5924.

(32) (a) Noodleman, L.; Norman, J. G., Jr. *J. Chem. Phys.* **1979**, *70*, 4903. (b) Noodleman, L. *J. Chem. Phys.* **1981**, *74*, 5737. (c) Noodleman, L.; Davidson, E. R. *Chem. Phys.* **1986**, *109*, 131. (d) Noodleman, L.; Case, D. A. *Adv. Inorg. Chem.* **1992**, *38*, 423.

(33) (a) Soda, T.; Kitagawa, Y.; Onishi, T.; Takano, Y.; Shigeta, Y.; Nagao, H.; Yoshioka, Y.; Yamaguchi, K. *Chem. Phys. Lett.* **2000**, *319*, 223. (b) Shoji, M.; Koizumi, K.; Kitagawa, Y.; Kawakami, T.; Yamanaka, S.; Okumura, M.; Yamaguchi, K. *Chem. Phys. Lett.* **2006**, *432*, 343.

(34) Llunell, M.; Casanova, D.; Cirera, J.; Bofill, M.; Alemany, P.; Alvarez, S.; Pinsky, M.; Avnir, D. *SHAPE program*, version 1.1b; Barcelona, 2003.